Samantha N. Sherman[1]
Department of Applied and Computational, Mathematics and Statistics, University of Notre Dame, Notre Dame, IN 46556
e-mail: ssherma1@nd.edu

Jonathan D. Hauenstein
Department of Applied and Computational Mathematics and Statistics, University of Notre Dame, Notre Dame, IN 46556
e-mail: hauenstein@nd.edu

Charles W. Wampler
Chemical and Materials System Lab, General Motors Global R&D, Warren, MI 48092
e-mail: charles.w.wampler@gm.com

Advances in the Theory of Planar Curve Cognates

Cognate linkages provide the useful property in mechanism design of having the same motion. This paper describes an approach for determining all coupler curve cognates for planar linkages with rotational joints. Although a prior compilation of six-bar cognates due to Dijksman purported to be a complete list, that analysis assumed, without proof, that cognates only arise by permuting link rotations. Our approach eliminates that assumption using arguments concerning the singular foci of the coupler curve to constrain a cognate search and then completing the analysis by solving a precision point problem. This analysis confirms that Dijksman's list for six-bars is comprehensive. As we further demonstrate on an eight-bar and a ten-bar example, the method greatly constrains the set of permutations of link rotations that can possibly lead to cognates, thereby facilitating the discovery of all cognates that arise in that manner. However, for these higher order linkages, the further step of using a precision point test to eliminate the possibility of any other cognates is still beyond our computational capabilities. [DOI: 10.1115/1.4052806]

Keywords: mechanism synthesis, theoretical kinematics

1 Introduction

By offering alternative mechanism dimensions that achieve the same motion, knowledge of cognates can be useful in mechanical design. Roberts's proof [1] that every planar four-bar coupler curve is generated by three distinct mechanisms was the first result in cognate theory. Much later, cognates were found for all the inversions of planar six-bar linkages, with Table 4 of Dijksman's book [2], based on Refs. [3,4], purporting to be a complete list. For a review of all the cognates known before the publication of that table, we refer the reader to Ref. [5] and the references in Ref. [6].

Dijksman's method of finding cognates included the following assumption [3]:

> We now make the assumption that the angular velocities occurring in all cognates to be found are permuted only …. It is then clear that not all permutations are permissible … In this way one can even try to forecast the number of cognates of six-bars.

For succinctness, we introduce the following terminology.

Definition A *permutation cognate* is one for which the rotations of its links are a permutation of the rotations of the original linkage, both measured in the world reference frame.

Dijksman's Conjecture All cognates for planar linkages with rotational links are permutation cognates.

This poses the question as to whether Dijksman's table is really complete. In short, three issues remain unresolved:

(1) Does Dijksman's Conjecture hold for four-bar and six-bar linkages?
(2) If it does hold, has Dijksman found all permissible permutations?
(3) For each permissible permutation, is there only one cognate (or, in one case, only one two-dimensional family of cognates)?

Given these open issues, only two rows in Dijksman's table can be considered complete:

- for four-bars, Roberts [1] settled the matter using arguments concerning the singular foci and nodal points of the coupler curve.
- Roth [7] gave a rigorous treatment of Stephenson-3 six-bars (and certain related geared linkages) by close examination of the coefficient equations of the coupler curve.

In addition to the above questions, we add:

(1) Can we find all permutation cognates more efficiently than exhaustive testing?
(2) Does Dijksman's Conjecture hold for higher-order linkages (eight-bars, ten-bars, etc.)?

In Refs. [8,9], we have previously shown how to answer Question 3 using a formulation wherein planar vectors are written as complex numbers. Given a linkage type and a permutation of the angles, these papers reduce the construction of the cognates for that permutation to solving a linear system of equations. This system either has no solutions (meaning that the permutation is invalid for generating cognates), has a unique solution, or has a linear set of solutions. By automating this method, one could also answer Question 2 by exhaustively testing every possible permutation. However, Question 1 remains open.

The present paper answers Question 1 definitively in a way that also lets us easily answer Question 2 without resorting to exhaustive testing. Moreover, our approach gives a highly effective answer to Question 4, thus facilitating the construction of all permutation cognates for higher-order linkages. The approach we use to settle Dijksman's conjecture for six-bars extends in principle to eight-bars and beyond, but the computations are currently beyond our capabilities, so Question 5 remains open. Nevertheless, we believe our method is a big step towards ultimately tackling that question.

Like Roberts [1] did for four-bars, for each linkage type, we start by determining the singular foci of the coupler curve. To do so, we use the methods of Refs. [10,11], supplemented by techniques from numerical algebraic geometry [12] as implemented in the software package BERTINI [13,14]. Since the singular foci belong to the coupler curve, not a specific linkage, all cognates must have the same singular foci with the same signatures. However, the singular foci alone do not completely determine the curve—recall that for four-bars, Roberts also considered the nodal points. To finish the job, our approach selects a few general points on the curve and solves the associated curve interpolation problem using numerical algebraic geometry. In this way, we find all curve cognates not

[1]Corresponding author.

Contributed by the Mechanisms and Robotics Committee of ASME for publication in the JOURNAL OF MECHANISMS AND ROBOTICS. Manuscript received June 15, 2021; final manuscript received October 11, 2021; published online November 16, 2021. Assoc. Editor: Andrew P. Murray.

just the permutation cognates. A side benefit is that the focal conditions already strongly limit the possible angle permutations, which is how we address Question 4.

To save space, we refer to the companion paper [9] for loop equations for all the six-bar inversions. Before treating these, we review the definition of a singular focus and describe how to compute the singular foci of a linkage. After first treating the Stephenson-2B linkage in detail, we summarize our results for all six-bars, omitting Watt-2 linkages because their coupler curves are the same as four-bars.

A caveat: throughout this paper, we restrict our attention to *general* linkages of the types we study. We do not rule out the possibility that additional curve cognates could appear in exceptional cases.

The rest of the paper is organized as follows. Section 2 reviews the definition of a singular foci and describes how to compute them, using the Stephenson-2B as an example. Section 3 summarizes the focal signatures for the four-bar, all six-bars, and one example each of an eight-bar and a ten-bar. It also details which permutations of the link rotations are compatible with these signatures, which is a necessary condition for a permutation cognate. In Sec. 4, to complete the analysis for six-bars, that is, to definitively answer Question 1, we find all cognates by appending an appropriate number of precision points to the focal point conditions and solve the system using numerical algebraic geometry. We summarize these results in Sec. 5.

2 Background

The problem of finding coupler curve cognates is closely connected to precision-point path synthesis problems. In the case of curve cognates, we are not given a finite set of points on the curve, but rather we wish to find all linkages that exactly reproduce the whole curve.

In principle, one way to solve the curve cognate problem is to use a complete solution to the maximal precision-point path synthesis problem. For example, only a finite number of distinct four-bars interpolate nine general points. Given a four-bar curve, we could select nine general points on it and find all four-bars interpolating them. These four-bars will separate into groups of cognates. In Ref. [15], complete solutions of the nine-point problem for four-bars were computed using numerical algebraic geometry, resulting in 1442 coupler curves that interpolate the points, each curve generated by three cognate linkages. This accords to Roberts's result that four-bars are triply generated. For six-bar linkages, such an approach becomes untenable since the precision-point problems are currently too big for current approaches.

For finding cognates, instead of choosing general points on the coupler curve, we can choose distinguished points associated with the coupler curve in order to make the synthesis problem easier. An advantageous choice is to select the points where the coupler curve approaches infinity, which is equivalent to finding the curve's singular foci. This approach is motivated by recalling that the ground pivots of a four-bar linkage coincide with two singular foci of its coupler curve. The maximal number of general precision points that can be specified for the path synthesis of a four-bar with specified ground pivots is just five, and the problem can be solved ab initio with a 96-path homotopy [16]. Furthermore, since we know the location of the third singular focus, that constraint reduces the maximal number of general precision points to just three, which allows one to find all cognates even more simply. Thus, this suggests that analyzing the singular foci of the coupler curves of six-bars and higher-order linkages might provide significant leverage in solving for cognates. Indeed, this will turn out to be the case, but first we must review the definition of singular foci and how to compute them.

2.1 Singular Foci and Isotropic Coordinates.

The notion that conics (parabolas, ellipses, and hyperbolas) have focal points is a familiar one. So too might one remember that as an ellipse is morphed into a circle, its two foci coalesce in to a single focus. This double focal point at the circle's center is an example of a singular focus, and it clearly tells us something fundamental about the circle. Similarly, the singular foci of coupler curves hold important information that can help us solve the riddle of curve cognates.

A general definition of singular foci can be found in Ref. [17], and examples of their application to linkages appear in Ref. [18]. We will make use of the treatment found in Refs. [10,11] which greatly simplifies computations through the use of isotropic coordinates. From a geometric viewpoint, both treatments involve analyzing how a curve meets infinity, whereas from an algebraic viewpoint, they involve analyzing the highest order terms of the coupler curve equation. This makes sense because near infinity, when variables get large, the highest order terms dominate the lower order ones. A fundamental difference of Refs. [17,18] as compared to Refs. [10,11] comes in how "infinity" is defined.

If one confines their analysis to the reals, the question of how a coupler curve reaches infinity is vacuous: links are finite, so the whole coupler curve must remain finite. For example, this is true of a circle. However, if we allow the coordinates of the curve to take on complex values, this picture completely changes. Fundamentally, this is because in the reals, the polynomial for squared distance from the origin, $x^2 + y^2$ has only a single zero, $(x, y) = (0, 0)$, whereas in complex space, any point with $y = \pm \mathbf{i}x$ is a zero. Because of this, there are points that stretch out to infinity in the complex plane while still satisfying a circle's equation. The same is true for any algebraic curve.

Let us call the two lines of points that are zero distance from the origin the isotropic lines. Their linear equations are $x + \mathbf{i}y = 0$ and $x - \mathbf{i}y = 0$. Since the fundamental property of a rigid link is that it preserves distance, it should not be too surprising that these lines hold a special significance. The classical treatment of singular foci takes a one-homogeneous approach wherein the open Euclidean plane is closed up by adding a line at infinity, having one point on that line for each slope a finite line can have. In a sense that can be made precise, two distinct parallel lines intersect at the point at infinity associated with their slope. This implies that all lines parallel to one of the isotropic lines meets it in the same point at infinity. These two isotropic points play a major role in the classical theory.

A more facile way of treating singular foci, and in many ways, a more convenient way of treating nearly all problems in planar linkages, is to use *isotropic coordinates*. This is almost identical to a complex-vector formulation of kinematics that treats any point (x, y) in the Euclidean plane as the point $p = x + \mathbf{i}y$ in the complex plane. To turn this into isotropic coordinates, we form a second coordinate $\bar{p} = x - \mathbf{i}y$ so that $(p, \bar{p})$ is just a linear change of coordinates from (x, y). When x and y are real, $\bar{p}$ is the complex conjugate of p, but this is no longer true when x or y has a nonzero imaginary part.

If we close up the Euclidean plane one-homogeneously, i.e., with a single line at infinity, all the lines parallel to the p-axis meet in one isotropic point, and all lines parallel to the $\bar{p}$-axis meet in the other one. But there is another way of closing up the plane that works to our advantage: add *two* lines at infinity, one parallel to each coordinate direction. This two-homogenization is done using the substitutions $p = P/w$ and $\bar{p} = \bar{P}/\hat{w}$, and clearing denominators. The new coordinates are written $([P, w], [\bar{P}, \hat{w}])$ and we do not allow $[P, w] = [0, 0]$ nor $[\bar{P}, \hat{w}] = [0, 0]$. The bracket notation means that only ratios matter: $[a, b]$ and $[\lambda a, \lambda b]$ for $\lambda \neq 0$ are considered the same point.

The bottom line (see Ref. [10] for more) is that after making this transformation, the coordinates of the singular foci are formed as the values of p where $\bar{p}$ hits infinity (i.e., where $\hat{w} = 0$) and vice versa for the values of $\bar{p}$. For the real curves we study here, if a term $\alpha p^j \bar{p}^k$ appears, so does its conjugate $\alpha^* p^k \bar{p}^j$. This means that $\bar{p}$ hits infinity in the complex conjugates of where p hits infinity, so in fact we just need to compute the p-coordinates. To do this for plane curve given by $f(p, \bar{p}) = 0$, make the substitution $\bar{p} = 1/\hat{w}$, clear denominators, set $\hat{w} = 0$, and solve for p. Or put more simply,

just cross out all terms of f except those with the highest power of $\bar{p}$ and then set $\bar{p} = 1$. The result is a simpler polynomial $g(p) = 0$ whose roots are the p-coordinates of the curve's singular foci. As a simple example, consider the equation $(p - c)(\bar{p} - c^*) - r^2 = 0$, which is a real circle with center c and radius r. Omitting lower-order terms in $\bar{p}$, we are left with $(p - c)\bar{p} = 0$, and setting $\bar{p} = 1$, we find that the singular focus of the circle is its center $p = c$. (More properly speaking, it is $(p, \bar{p}) = (c, c^*)$.)

2.2 Computing Singular Foci. To find singular foci following the prescription earlier, we need a curve's coupler curve equation in the form $f(p, \bar{p}) = 0$. In Ref. [10], it is shown how to carry this through using the Dixon determinant formulation from Ref. [19] to eliminate rotation angles from the kinematic loop equations. In Ref. [11], the singular foci are found by direct computations on the loop equations without elimination, which yields additional information about the rotations associated with the singular foci. To automate this, we follow the paradigm of numerical elimination theory [14,20] in numerical algebraic geometry and use the software package BERTINI [13,14]. This approach avoids any trouble with extraneous roots, which is a possibility when using the Dixon determinant. Furthermore, the information about rotations further constrains the possible cognates, making our search for cognates more efficient.

Consider an N-link mechanism which has one degree-of-freedom (DOF). Thus, N must be even and the linkage has $N/2 - 1$ loop equations together with an equation for the location of the coupler point p relative to the origin. To write relations directly in isotropic coordinates, we use a complex-plane formulation wherein translations become addition and rotations are multiplication by a complex number of unit magnitude. Specifically, letting Θ_j be the angle of rotation of link j with respect to ground, $\theta_j = e^{i\Theta_j}$ is its complex rotation. Fixing link 0 as the ground link, there are $N - 1$ rotations θ_j for the moving links. The loop equations and coupler point equation can be written relative to the origin in the form

$$a_{k0} + \sum_{j=1}^{N-1} a_{kj}\theta_j + a_{kN}p = 0, \quad k = 1, \ldots, N/2 \tag{1}$$

where each a_{kj} is a complex vector between two points of link j in its reference position. (Since the a_{kj} are complex, any offset angle that would result from choosing a different reference orientation can be absorbed into these coefficients.) To work in Cartesian coordinates, one would take the real and imaginary parts of these equations, but to work in isotropic coordinates we keep them as is and merely introduce the conjugate equations

$$a^*_{k0} + \sum_{j=1}^{N-1} a^*_{kj}\bar{\theta}_j + a^*_{kN}\bar{p} = 0, \quad k = 1, \ldots, N/2 \tag{2}$$

along with the unit-length equations

$$\theta_j\bar{\theta}_j = 1, \quad j = 1, \ldots, N - 1 \tag{3}$$

Together, Eqs. (1)–(3) form a system of $2N - 1$ equations in the $2N$ variables $\{(\theta_1, \ldots, \theta_{N-1}, p), (\bar{\theta}_1, \ldots, \bar{\theta}_{N-1}, \bar{p})\}$, describing the linkage's 1-DOF motion.

As discussed in Sec. 2.1, the singular foci are the points where the coupler curve approaches infinity in $\bar{p}$. Because we have not eliminated the rotation angles, we include them in our two-homogenization procedure by substituting $\bar{p} = 1/\hat{w}$ as before while also rescaling $\bar{\theta}_j = \hat{\theta}_j/\hat{w}$ for $j = 1, \ldots, N - 1$. Clearing denominators in Eqs. (2) and (3) yields

$$a^*_{k0}\hat{w} + \sum_{j=1}^{N-1} a^*_{kj}\hat{\theta}_j + a^*_{kN} = 0, \quad k = 1, \ldots, N/2 \tag{4}$$

$$\theta_j\hat{\theta}_j = \hat{w}, \quad j = 1, \ldots, N - 1 \tag{5}$$

The singular foci are given by where the solution curve of the system (1), (4), and (5) intersects $\hat{w} = 0$. It turns out that the system obtained by merely substituting $\hat{w} = 0$ may have additional solutions which do not arise as limits of the coupler curve. So, instead of solving that system directly, we use a homotopy that reveals how finite arcs of the curve approach infinity. This is accomplished by slicing with a hyperplane to get finitely-many points and then following the paths starting from these points as the hyperplane is moved smoothly to infinity.

Specifically, we start by appending the equation

$$\ell(\hat{w}) := \hat{w} - c = 0 \tag{6}$$

where the complex coefficient c is chosen random for genericity. Given all the coefficients a_{kj} and c, the system (1), (4)–(6) consists of $2N$ polynomials in $2N$ unknowns that is easily solved using BERTINI for relevant sizes of N.

Once the finite solutions are known, they become start points corresponding with $t = 1$ for the homotopy that deforms the slicing hyperplane $\ell(\hat{w})$ to the hyperplane at infinity $\hat{w} = 0$ as $t \to 0$, namely

$$h(\hat{w}, t) := t\ell(\hat{w}) + (1 - t)\hat{w} = \hat{w} - t \cdot c = 0 \tag{7}$$

The full set of equations for the homotopy is Eqs. (1), (4), (5), and (7). Given the start points for the homotopy, the solution paths can be tracked, for example, using a user-defined homotopy in BERTINI. The endpoints at $t = 0$ are the values of p for the singular foci. We also may observe the multiplicities of the singular foci by the number of paths that converge to each. Furthermore, notice that at $t = 0$, where $\hat{w} = 0$, each corresponding unit length equation (5) has become $\theta_j\hat{\theta}_j = 0$ so that either $\theta_j = 0$ or $\hat{\theta}_j = 0$ for every $j = 1, \ldots, N - 1$. It is easily observed that both cannot be zero since that does not leave enough freedoms to satisfy all the remaining equations. Therefore, the pattern of which $N - 1$ variables among $\{\theta_j, \hat{\theta}_j, j = 1, \ldots, N - 1\}$ is zero at each singular focus becomes an additional signature of the focus.

This homotopy-based approach computes the singular foci as numerical values that are dependent on the input coefficients a_{kj}. In some cases, symbolic formulas for each singular focus can be trivially observed from the numerical values such as when a singular focus is a ground pivot. Explicit symbolic expressions of the singular foci are not required to find permutation cognates but to settle the existence of any other cognates, they become essential. One approach to deriving is to employ exactness recovery methods [21] to determine symbolic expressions directly from numerical computations. Alternatively, one can use a computer algebra package, taking advantage of the knowledge of which rotations vanish at each singular focus to simplify expressions.

2.3 Singular Foci of Stephenson-2B. To illustrate the approach in Sec. 2.2 for computing singular foci, we consider computing the singular foci of the Stephenson-2B six-bar linkage, shown in Fig. 1. In this figure and the rest, we draw the linkage in a reference pose where all link rotations are zero (Remember that any offset angle can be absorbed into the link vectors.). In any other pose along the coupler curve, link vector a_1 rotates to $\theta_1 a_1$ and similarly for the rest. Each loop equation for the link is just a sum of these rotated vectors. Referring to the notation in Fig. 1, after making the substitutions for $\bar{p}$ and $\bar{\theta}_j$, and clearing denominators, the system consisting of the loop, coupler point, and unit length equations is

$$\begin{aligned}
0 &= (a_0 - b_0) + a_1\theta_1 + a_2\theta_2 + a_3\theta_3 - a_4\theta_4 \\
0 &= (a^*_0 - b^*_0)\hat{w} + a^*_1\hat{\theta}_1 + a^*_2\hat{\theta}_2 + a^*_3\hat{\theta}_3 - a^*_4\hat{\theta}_4 \\
0 &= b_2\theta_2 + a_3\theta_3 + b_4\theta_4 + a_5\theta_5 \\
0 &= b^*_2\hat{\theta}_2 + a^*_3\hat{\theta}_3 + b^*_4\hat{\theta}_4 + a^*_5\hat{\theta}_5 \\
p &= a_0 + a_1\theta_1 + c_2\theta_2 \\
1 &= a^*_0\hat{w} + a^*_1\hat{\theta}_1 + c^*_2\hat{\theta}_2 \\
0 &= \theta_j\hat{\theta}_j - \hat{w} \quad j = 1, \ldots, 5
\end{aligned}$$

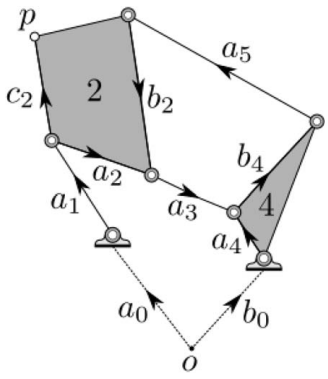

Fig. 1 Stephenson-2B mechanism

To compute the start points of the homotopy, we append the linear equation (6) and use BERTINI to compute the nine solutions. Replacing Eq. (6) by (7) and tracking the homotopy paths emanating from the nine points, yields the singular foci. Symbolic expressions for the singular foci are shown in Table 1 along with the corresponding rotations that vanished at infinity. Multiplicities greater than one are explicitly noted. For example, in the first row of Table 1, $b_0 \times 3$ means that three paths end at b_0 with the same set of vanishing rotations. Three paths also end at a_0 but different sets of rotations vanish for each, so the multiplicity with respect to each set of vanishing rotations is one while the total multiplicity of a_0 is three. This analysis shows that the two ground pivots are both singular foci with multiplicity 3, but the extra information provided by the vanishing rotations show that these singular foci are geometrically different from each other as well as the others. As we will see next, this shows that every Stephenson-2B cognate linkage must have the same ground pivots.

3 Focal Signatures and Permutations

For linkage type, the term *focal signature* consists of the number of singular foci, the distinct patterns of vanishing rotations at each singular focus, and the multiplicity of each pattern. The computational approach in Sec. 2.2 yields all this information. For the Stephenson-2B, this is the information in Table 1 except the explicit symbolic formulas. It tells us that there are five singular foci: two with multiplicity 3 and three each having multiplicity one. Furthermore, one of the multiplicity 3 singular foci comes from a multiplicity 3 vanishing pattern, whereas the other one comes from three distinct vanishing patterns each of multiplicity 1. Table 2 lists the focal signature information for the four-bar and all six-bar types. For easier reading, it only shows the vanishing rotations in θ_j for $j = 1, \ldots, N-1$ since one immediately knows from this list that the complementary $\hat{\theta}_k$ vanish. As can be observed in that table, it is possible for a singular focus to have different multiplicities with respect to different vanishing rotations. In particular, this occurs for singular focus b_0 of the Watt-1A and Stephenson-2A linkages.

Table 1 Rotations that vanish and corresponding singular foci for Stephenson-2B

Vanishing rotations	Singular foci and multiplicity
$\theta_2, \theta_3, \theta_4, \theta_5, \hat{\theta}_1$	$b_0 \times 3$
$\theta_1, \theta_2, \theta_4, \hat{\theta}_3, \hat{\theta}_5$	a_0
$\theta_1, \theta_2, \theta_5, \hat{\theta}_3, \hat{\theta}_4$	a_0
$\theta_1, \theta_2, \theta_3, \hat{\theta}_4, \hat{\theta}_5$	a_0
$\theta_1, \theta_3, \theta_4, \hat{\theta}_2, \hat{\theta}_5$	$\dfrac{a_0 \cdot a_2 - a_0 \cdot c_2 + b_0 \cdot c_2}{a_2}$
$\theta_1, \theta_4, \theta_5, \hat{\theta}_2, \hat{\theta}_3$	$\dfrac{a_0 \cdot a_2 - a_0 \cdot b_2 - a_0 \cdot c_2 + b_0 \cdot c_2}{a_2 - b_2}$
$\theta_1, \theta_3, \theta_5, \hat{\theta}_2, \hat{\theta}_4$	$\dfrac{a_0 \cdot a_2 \cdot b_4 + a_0 \cdot a_4 \cdot b_2 - a_0 \cdot b_4 \cdot c_2 + b_0 \cdot b_4 \cdot c_2}{a_2 \cdot b_4 + a_4 \cdot b_2}$

Table 2 Vanishing rotations and singular foci for the four-bar and six-bar mechanisms

Mechanism	Vanishing rotations	Singular foci and multiplicity
4-Bar	θ_1, θ_2	a_0
	θ_2, θ_3	b_0
	θ_1, θ_2	$(a_0 \cdot a_2 + b_2 \cdot b_0 - b_2 \cdot a_0)/a_2$
Watt-1A	$\theta_2, \theta_3, \theta_4, \theta_5$	$b_0 \times 2$
	$\theta_1, \theta_3, \theta_5$	b_0
	$\theta_1, \theta_2, \theta_5$	$(a_0 \cdot a_3 + a_0 \cdot b_3 - b_0 \cdot b_3)/a_3$
	$\theta_1, \theta_3, \theta_4$	$(a_2 \cdot a_5 \cdot b_0 + a_0 \cdot b_2 \cdot b_5 - b_0 \cdot b_2 \cdot b_5)/(a_2 \cdot a_5)$
	θ_4, θ_5	roots of a quadratic
Watt-1B	$\theta_2, \theta_3, \theta_4, \theta_5$	$b_0 \times 2$
	$\theta_1, \theta_2, \theta_4$	a_0
	$\theta_1, \theta_3, \theta_4$	$(a_2 \cdot b_0 - a_0 \cdot b_2 + b_0 \cdot b_2)/a_2$
	$\theta_1, \theta_3, \theta_5$	$(a_2 \cdot a_4 \cdot b_0 + a_0 \cdot b_2 \cdot b_4 - b_0 \cdot b_2 \cdot b_4)/(a_2 \cdot a_4)$
	$\theta_1, \theta_2, \theta_5$	$(a_0 \cdot a_3 \cdot a_4 + a_0 \cdot a_4 \cdot b_3 + a_0 \cdot b_3 \cdot b_4 - a_4 \cdot b_0 \cdot b_3 - b_0 \cdot b_3 \cdot b_4)/(a_3 \cdot a_4)$
	θ_4, θ_5	roots of a quadratic
Stephenson-1	$\theta_1, \theta_3, \theta_5$	b_0
	$\theta_2, \theta_3, \theta_5$	b_0
	$\theta_1, \theta_2, \theta_5$	$(a_0 \cdot a_3 + a_0 \cdot b_3 - b_0 \cdot b_3)/a_3$
	$\theta_1, \theta_3, \theta_4$	$(a_0 \cdot b_5 + a_5 \cdot b_0 - b_0 \cdot b_5)/a_5$
	$\theta_2, \theta_3, \theta_4$	$(a_1 \cdot a_5 \cdot b_0 + a_0 \cdot b_1 \cdot b_5 - b_0 \cdot b_1 \cdot b_5)/(a_1 \cdot a_5)$
	θ_4, θ_5	roots of a cubic
Stephenson-2A	$\theta_2, \theta_3, \theta_4, \theta_5$	$b_0 \times 3$
	$\theta_1, \theta_4, \theta_5$	b_0
	$\theta_1, \theta_2, \theta_5$	a_0
	$\theta_1, \theta_3, \theta_5$	$(a_0 \cdot a_4 \cdot b_2 - a_0 \cdot b_2 \cdot b_4 + a_2 \cdot b_0 \cdot b_4 + b_0 \cdot b_2 \cdot b_4)/(a_2 \cdot b_4 + a_4 \cdot b_2)$
	$\theta_1, \theta_3, \theta_4$	$(a_2 \cdot a_5 \cdot b_0 + a_0 \cdot b_2 \cdot b_5 - b_0 \cdot b_2 \cdot b_5)/(a_2 \cdot a_5)$
	$\theta_1, \theta_2, \theta_4$	$(a_5 \cdot b_0 - a_0 \cdot b_5 + b_0 \cdot b_5)/a_5$
Stephenson-2B	$\theta_2, \theta_3, \theta_4, \theta_5$	$b_0 \times 3$
	$\theta_1, \theta_2, \theta_4$	a_0
	$\theta_1, \theta_2, \theta_5$	a_0
	$\theta_1, \theta_2, \theta_3$	a_0
	$\theta_1, \theta_3, \theta_4$	$(a_0 \cdot a_2 - a_0 \cdot c_2 + b_0 \cdot c_2)/a_2$
	$\theta_1, \theta_4, \theta_5$	$(a_0 \cdot a_2 - a_0 \cdot b_2 - a_0 \cdot c_2 + b_0 \cdot c_2)/(a_2 - b_2)$
	$\theta_1, \theta_3, \theta_5$	$(a_0 \cdot a_2 \cdot b_4 + a_0 \cdot a_4 \cdot b_2 - a_0 \cdot b_4 \cdot c_2 + b_0 \cdot b_4 \cdot c_2)/(a_2 \cdot b_4 + a_4 \cdot b_2)$
Stephenson-3	$\theta_1, \theta_2, \theta_5$	a_0
	$\theta_2, \theta_3, \theta_5$	b_0
	θ_4, θ_5	$c_0 \times 3$
	$\theta_2, \theta_3, \theta_4$	$(a_5 \cdot c_0 + b_0 \cdot b_5 - b_5 \cdot c_0)/a_5$
	$\theta_1, \theta_2, \theta_4$	$(a_5 \cdot c_0 + a_0 \cdot b_5 - b_5 \cdot co)/a_5$
	$\theta_1, \theta_3, \theta_5$	$(a_2 \cdot b_0 - a_0 \cdot b_2)/(a_2 - b_2)$
	$\theta_1, \theta_3, \theta_4$	$(a_2 \cdot b_0 \cdot b_5 - a_0 \cdot b_2 \cdot b_5 + a_2 \cdot a_5 \cdot c_0 - a_5 \cdot b_2 \cdot c_0 - a_2 \cdot b_5 \cdot c_0 + b_2 \cdot b_5 \cdot c_0)/(a_5 \cdot (a_2 - b_2))$

If a cognate is a permutation cognate, the permutation of the angles will permute the patterns of rotations that vanish where the coupler curve hits infinity. But this focal signature is a generic property of the linkage, so it cannot change. Only angle permutations that preserve the focal signature are candidates for permutation cognates. Applying any two signature-preserving permutations in succession still preserves the signature, so the collection of all such permutations forms a group.

Preservation of the focal signature is a necessary but not sufficient condition for an angle permutation to give a valid cognate. The final check is to apply the methods from Refs. [8,9] to see if the signature-preserving permutations are consistent with

preserving the system of loop and coupler point equations. We will find that except in the case of the four-bar, the signature-preserving permutations are a small subset of full set of permutations among the moving links, i.e., for $n \geq 6$, each n-link mechanism type has many fewer than $(n-1)!$ signature-preserving permutations. We will give the details in the following subsections, starting with our running example, the Stephenson-2B.

3.1 Group Notation. Our discussion will benefit from using notation from the theory of groups. A two-way symmetry, which arises from a transposition, is denoted $\mathbb{Z}_2$. For example, swapping rotations θ_1 and θ_2, which corresponds with the transposition denoted $\theta_1 \leftrightarrow \theta_2$, yield a two-symmetry group action $\mathbb{Z}_2$. If k independent transpositions act on distinct elements, then the resulting group of size 2^k is denoted

$$\underbrace{\mathbb{Z}_2 \times \cdots \times \mathbb{Z}_2}_{k \text{ times}}$$

For example, the three transpositions $\theta_1 \leftrightarrow \theta_2$, $\theta_3 \leftrightarrow \theta_4$, and $\theta_5 \leftrightarrow \theta_6$ are applied to distinct elements so the resulting group action is $\mathbb{Z}_2 \times \mathbb{Z}_2 \times \mathbb{Z}_2$, which has order $2^3 = 8$.

A three-way symmetry arises from two transpositions that have an element in common, which is denoted S_3 and has order $3! = 6$. For example, the transpositions $\theta_1 \leftrightarrow \theta_2$ and $\theta_1 \leftrightarrow \theta_3$ have one element in common, namely θ_1, so this corresponds with the three-way symmetry group S_3. Finally, the product $S_3 \times \mathbb{Z}_2$ has order $3! \cdot 2 = 12$ and arises from three permutations, two which have one element in common with the third one having distinct elements, e.g., $\theta_1 \leftrightarrow \theta_2$, $\theta_1 \leftrightarrow \theta_3$, and $\theta_4 \leftrightarrow \theta_5$.

Every permutation group includes the trivial permutation where nothing is changed. We will refer to any other permutation as *nontrivial*.

3.2 Valid Permutations of Stephenson-2B. Using Table 1, we can determine which permutations are valid. As noted in Sec. 2.3, there are three types of singular foci: ground pivot a_0, ground pivot b_0, and the three singular foci of multiplicity 1. Hence, all valid permutations must keep the two ground pivots fixed, but the three singular foci of multiplicity 1 may permute among themselves.

From b_0, one sees that θ_1 cannot permute with any other rotation as $\hat{\theta}_1$ is the unique $\hat{\theta}_j$ vanishing at b_0. Since θ_1 cannot permute and θ_2 is the only other rotation that appears in each of the three sets of rotations for a_0, θ_2 also cannot permute. Therefore, the two ground pivots have shown that the only possible permutations are among θ_3, θ_4, and θ_5. Checking transpositions $\theta_3 \leftrightarrow \theta_4$ and $\theta_4 \leftrightarrow \theta_5$ separately shows that the vanishing structure for the ground pivots and one of the other singular foci of multiplicity 1 are maintained while transposing the other two singular foci of multiplicity 1. Hence, this yields a three-way symmetry among θ_3, θ_4, and θ_5 showing that the group action on the Stephenson-2B cognates corresponds with S_3. Note that since links 3 and 5 are both binary links connected between links 2 and 4, they are topologically equivalent, so the transposition $\theta_3 \leftrightarrow \theta_5$ corresponds with a relabeling of the mechanism rather than a new cognate. Accordingly, only three of the six permutations in S_3 have the potential to yield unique mechanisms. As found in Ref. [9], these are in fact valid permutation cognates.

3.3 Four-Bar Valid Permutations. As Roberts [1] identified, the three singular foci of the four-bar can be permuted in any way which corresponds to any permutation of the three rotations. Hence, the three-way symmetry shows that the group action on the rotations of the four-bar corresponds with S_3. Considering Fig. 2(*a*), the transposition $\theta_1 \leftrightarrow \theta_3$ corresponds with relabeling so only three of the six permutations in S_3 can produce unique mechanisms. These are the permutation cognates found by Roberts [1].

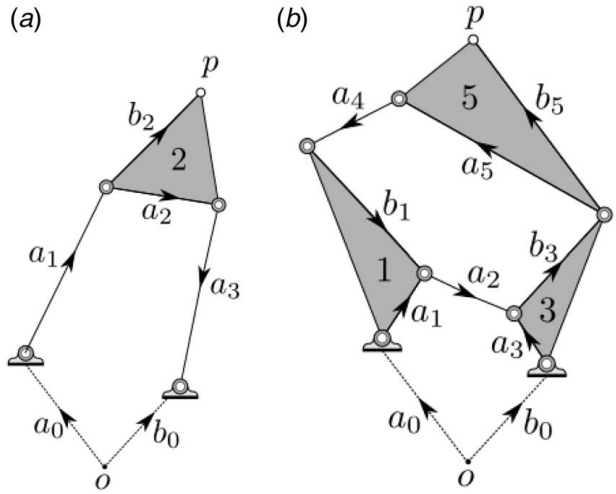

Fig. 2 (*a*) Four-bar and (*b*) Stephenson-1

3.4 Stephenson-1 Valid Permutations. The only valid nontrivial permutation of rotations for the Stephenson-1 is the transposition $\theta_1 \leftrightarrow \theta_2$. Hence, the group action corresponds with $\mathbb{Z}_2$. This action gives a permutation cognate.

3.5 Stephenson-2A Valid Permutations. The group of signature-preserving permutations for Stephenson-2A is $\mathbb{Z}_2 \times \mathbb{Z}_2$ generated by the two transpositions $\theta_2 \leftrightarrow \theta_3$ and $\theta_4 \leftrightarrow \theta_5$ yielding permutation cognates (Fig. 3).

3.6 Stephenson-3 Valid Permutations. Considering Fig. 4, Roth [7] determined that the cognates of the Stephenson-3 mechanism are generated by applying Roberts cognates to the four-bar formed by links 0-1-2-3 and a skew pantograph transformation to links 10-4-5 as discussed in Ref. [8]. The results of the computation from Sec. 2.2 match those previously known results as follows. First, the group of valid permutations of the Stephenson-3 mechanism corresponds with $S_3 \times \mathbb{Z}_2$ where the S_3 arises from a three-way symmetry of the rotations θ_1, θ_2, and θ_3 while the $\mathbb{Z}_2$ arises from the transposition $\theta_4 \leftrightarrow \theta_5$. Finally, as in the case of the four-bar, the group S_3 can only produce three unique mechanisms due to relabeling.

3.7 Watt-1A Valid Permutations. For the Watt-1A, the only signature-preserving permutation is the trivial one. However, the

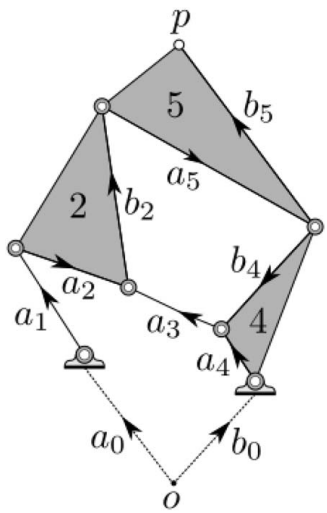

Fig. 3 Stephenson-2A

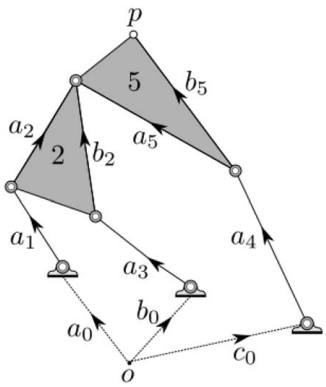

Fig. 4 Stephenson-3

Watt-1A is unique among the six-bars as it has a two-dimensional family of cognates (Fig. 5).

3.8 Watt-1B Valid Permutations. The group of signature-preserving permutations for Watt-1B is $\mathbb{Z}_2 \times \mathbb{Z}_2$ generated by the transpositions $\theta_2 \leftrightarrow \theta_3$ and $\theta_4 \leftrightarrow \theta_5$. These yield permutation cognates.

3.9 Valid Permutations of An Eight-Bar Mechanism. Whereas our analysis of the six-bars confirms that Dijksman found all permutation cognates, the equivalent question for higher-order linkages has never been addressed. An exhaustive check of all possible permutations for an eight-bar would have $7! = 5040$ cases to check. (The ground link is fixed, so an n-link mechanism has $(n-1)$ link angles that might permute.) The necessity of preserving the focal signature greatly reduces the task. We illustrate this fact by treating the eight-bar shown in Fig. 6 followed by a ten-bar in the next section.

For this eight-bar, the slice (6) gives 23 finite points on the coupler curve, which are then tracked to infinity using Eq. (7) to find the singular foci. Nine are distinct singular foci with multiplicity 1 corresponding to the following sets of vanishing rotations:

$$\begin{array}{lll} \{\theta_1, \theta_2, \theta_4, \theta_7\}, & \{\theta_1, \theta_2, \theta_5, \theta_6\}, & \{\theta_1, \theta_2, \theta_5, \theta_7\} \\ \{\theta_1, \theta_3, \theta_4, \theta_6\}, & \{\theta_1, \theta_3, \theta_4, \theta_7\}, & \{\theta_1, \theta_3, \theta_5, \theta_6\} \\ \{\theta_2, \theta_3, \theta_4, \theta_6\}, & \{\theta_2, \theta_3, \theta_4, \theta_7\}, & \{\theta_2, \theta_3, \theta_5, \theta_6\} \end{array} \tag{8}$$

Two more are located at the ground pivot b_0 but with different vanishing rotations:

$$\{\theta_1, \theta_3, \theta_5, \theta_7\} \quad \text{and} \quad \{\theta_2, \theta_3, \theta_5, \theta_7\} \tag{9}$$

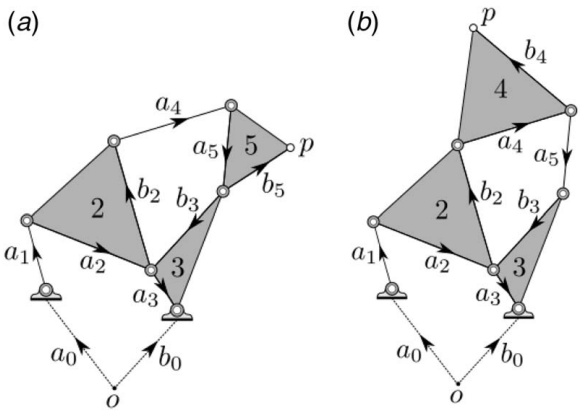

Fig. 5 (*a*) Watt-1A and (*b*) Watt-1B

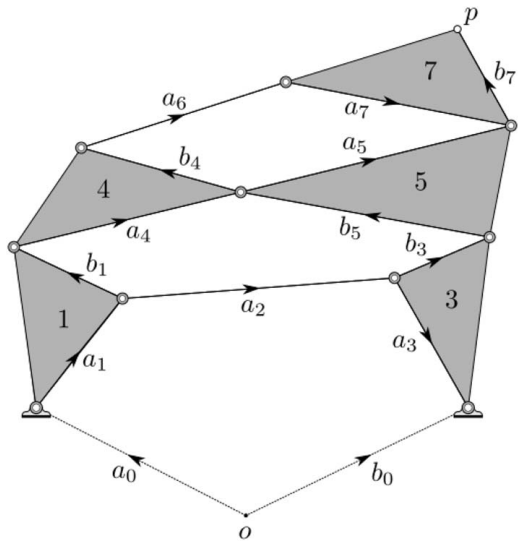

Fig. 6 An eight-bar mechanism

Finally, there are two distinct singular foci that each have multiplicity 6 arising from the following vanishing rotations:

$$\{\theta_4, \theta_5, \theta_6, \theta_7\} \quad \text{and} \quad \{\theta_6, \theta_7\} \tag{10}$$

From Eq. (10), one sees that the set of rotations decomposes into three sets which could permute among themselves, namely $\{\theta_1, \theta_2, \theta_3\}$, $\{\theta_4, \theta_5\}$, and $\{\theta_6, \theta_7\}$. Now, Eq. (9) refines this since θ_5 and θ_7 appear while θ_4 and θ_6 do not appear showing that θ_4, θ_5, θ_6, and θ_7 must all not permute. Moreover, since θ_3 appears in both collections while θ_1 and θ_2 only appear once, θ_3 must not permute yielding the only possible permutation is the transposition $\theta_1 \leftrightarrow \theta_2$. Checking Eq. (8) shows that this transposition keeps the first row invariant while the second and third rows interchange meaning that this is permutation preserves the focal signature. The group action on the rotations corresponds with $\mathbb{Z}_2$ of order 2.

By computing the focal signature, we have reduced the complete analysis of permutation cognates from 5040 cases to just 2. The trivial permutation and the transposition $\theta_1 \leftrightarrow \theta_2$ each give a unique mechanism: the original one in Fig. 6 and its cognate shown in Ref. [8].

3.10 Valid Permutations of a Ten-Bar Mechanism. The final example is to determine the valid permutations of the ten-bar linkage in Ref. [22] and shown in Fig. 7. Tracking 56 paths for this ten-bar linkage produced the following structure regarding vanishing rotations and multiplicity. There are eight distinct singular foci with multiplicity 1 corresponding to the following sets of vanishing rotations:

$$\begin{array}{ll} \{\theta_1, \theta_2, \theta_3, \theta_5, \theta_7\}, & \{\theta_1, \theta_2, \theta_3, \theta_7, \theta_8\} \\ \{\theta_1, \theta_2, \theta_4, \theta_5, \theta_7\}, & \{\theta_1, \theta_2, \theta_4, \theta_7, \theta_8\} \\ \{\theta_2, \theta_3, \theta_5, \theta_6, \theta_7\}, & \{\theta_2, \theta_3, \theta_6, \theta_7, \theta_8\} \\ \{\theta_2, \theta_4, \theta_5, \theta_6, \theta_7\}, & \{\theta_2, \theta_4, \theta_6, \theta_7, \theta_8\} \end{array} \tag{11}$$

There are four distinct singular foci each with multiplicity 2 that arise from two distinct sets of vanishing rotations with multiplicity 1. The first one in the following list corresponds with ground pivot b_0:

$$\begin{array}{lll} \{\theta_1, \theta_2, \theta_4, \theta_5, \theta_9\} & \text{and} & \{\theta_2, \theta_4, \theta_5, \theta_6, \theta_9\} \\ \{\theta_1, \theta_2, \theta_4, \theta_8, \theta_9\} & \text{and} & \{\theta_2, \theta_4, \theta_6, \theta_8, \theta_9\} \\ \{\theta_1, \theta_2, \theta_3, \theta_8, \theta_9\} & \text{and} & \{\theta_2, \theta_3, \theta_6, \theta_8, \theta_9\} \\ \{\theta_1, \theta_2, \theta_3, \theta_5, \theta_9\} & \text{and} & \{\theta_2, \theta_3, \theta_5, \theta_6, \theta_9\} \end{array} \tag{12}$$

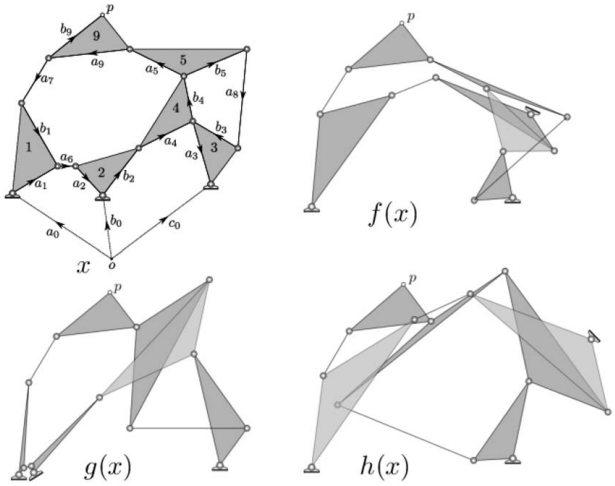

Fig. 7 Original ten-bar mechanism *x* and three cognates *f*(x), *g*(x), and *h*(x)

Next, there are five distinct singular foci that arise from a single set of vanishing rotations of multiplicity 4. The first one in the following list corresponds with the ground pivot c_0:

$$\{\theta_3, \theta_4, \theta_5, \theta_8, \theta_9\}, \quad \{\theta_3, \theta_4, \theta_5, \theta_7, \theta_8\}$$
$$\{\theta_1, \theta_6, \theta_9\}, \quad \{\theta_5, \theta_7, \theta_8\}, \quad \{\theta_5, \theta_8, \theta_9\} \tag{13}$$

Finally, there is a singular focus that arises from the following set of vanishing rotations of multiplicity 20:

$$\{\theta_7, \theta_9\} \tag{14}$$

This focal signature limits the possible permutation cognates. First, Eqs. (13) and (14) show that θ_7 and θ_9 must remain fixed. Next, since θ_2 is the only rotation in every collection in Eq. (11), it also cannot permute. Of the six remaining, namely θ_1, θ_3, θ_4, θ_5, θ_6, and θ_8, the bottom row in Eq. (13) shows that the only possible permutations must arise from the three transpositions $\theta_1 \leftrightarrow \theta_6$, $\theta_3 \leftrightarrow \theta_4$, and $\theta_5 \leftrightarrow \theta_8$. Each of these transpositions preserves the focal signature so that the corresponding group action on the rotations is $\mathbb{Z}_2 \times \mathbb{Z}_2 \times \mathbb{Z}_2$. This analysis has reduced the number of permutations to check from $9! = 362,880$ to just 4, the trivial permutation and three transpositions.

For the four cases remaining, the methods described in the companion papers [8,9] can compute the permutation cognates. The transpositions $\theta_3 \leftrightarrow \theta_4$ and $\theta_5 \leftrightarrow \theta_8$ along with the combination of both of these generate three distinct cognates of the original mechanism which are denoted $f(x)$, $g(x)$, and $h(x)$, respectively, in Fig. 7. Table 3 together with (15) contain explicit formulas for the cognates while Table 4 lists numerical values (rounded to four decimal places).

$$\gamma_1 = \frac{a_0a_4 + b_4b_0 - b_4c_0 - c_0a_4}{a_4(a_0 - b_0)}, \quad \gamma_2 = -\frac{b_4}{a_4}, \quad \gamma_3 = -\frac{a_3}{b_3}$$
$$\zeta_1 = \frac{a_0a_3b_5 - a_3b_0b_5 - a_5b_0b_3 + a_5b_3c_0}{a_3b_5(a_0 - b_0)}$$
$$\zeta_2 = \frac{a_3b_5 + a_5b_3}{a_3b_5}, \quad \zeta_3 = \frac{b_5 - a_5}{b_5}$$
$$\delta_1 = \frac{a_0a_4b_5 - a_5b_0b_4 - a_4b_5c_0 + a_5b_4c_0 + b_0b_4b_5 - b_4b_5c_0}{a_4b_5(a_0 - b_0)}$$
$$\delta_2 = \frac{b_4(a_5 - b_5)}{a_4b_5}, \quad \delta_3 = -\frac{a_3b_5 + a_5b_3}{b_3b_5} \tag{15}$$

Unlike the other signature-preserving permutations, the transposition $\theta_1 \leftrightarrow \theta_6$ results in an inconsistent system. Therefore, there does not exist a cognate that arises by simply permuting the angular velocities θ_1 and θ_6.

Table 3 Link rotations and link parameters for a ten-bar mechanism (x) and three curve cognates (*f*(x), *g*(x), *h*(x))

	Cognate	x	$f(x)$	$g(x)$	$h(x)$
Link rotations	1	θ_1	θ_1	θ_1	θ_1
	2	θ_2	θ_2	θ_2	θ_2
	3	θ_3	θ_4	θ_3	θ_4
	4	θ_4	θ_3	θ_4	θ_3
	5	θ_5	θ_5	θ_8	θ_8
	6	θ_6	θ_6	θ_6	θ_6
	7	θ_7	θ_7	θ_7	θ_7
	8	θ_8	θ_8	θ_5	θ_5
	9	θ_9	θ_9	θ_9	θ_9
Link parameters	0	a_0	a_0	a_0	a_0
		b_0	$c_0 + \gamma_2(b_0 - c_0)$	$c_0 + \zeta_2(b_0 - c_0)$	$c_0 + \delta_2(b_0 - c_0)$
		c_0	c_0	c_0	c_0
	1	a_1	$\gamma_1 a_1$	$\zeta_1 a_1$	$\delta_1 a_1$
		b_1	$b_1 + a_1(\gamma_1 - 1)$	$b_1 + a_1(\zeta_1 - 1)$	$b_1 + a_1(\delta_1 - 1)$
	2	a_2	$\gamma_1 a_2$	$\zeta_1 a_2$	$\delta_1 a_2$
		b_2	$\gamma_2 b_2$	$\zeta_2 b_2$	$\delta_2 b_2$
	3	a_3	$-b_4$	$\zeta_2 a_3$	$\delta_2 a_4$
		b_3	$\gamma_3 b_4$	$\zeta_3 b_3$	$\delta_3 b_4$
	4	a_4	$\gamma_2 a_3$	$\zeta_2 a_4$	$\delta_2 a_3$
		b_4	$-a_3$	$\zeta_3 b_4$	$\delta_3 b_3$
	5	a_5	a_5	$a_8(\zeta_3 - 1)$	$-a_5 a_8 / b_5$
		b_5	$\gamma_3 b_5$	$\zeta_3 a_8$	$\delta_3 a_8$
	6	a_6	$\gamma_1 a_6$	$\zeta_1 a_6$	$\delta_1 a_6$
	7	a_7	a_7	a_7	a_7
	8	a_8	$\gamma_3 a_8$	$b_5 - a_5$	$\delta_3 b_5$
	9	a_9	a_9	a_9	a_9
		b_9	b_9	b_9	b_9

Table 4 Ten bar linkage and cognate parameters where $i = \sqrt{-1}$

	Original	Swap 3–4	Swap 5–8	Swap 3–4 & 5–8
a_0	$0.0 + 0.0i$	$0.0000 + 0.0000i$	$0.0000 + 0.0000i$	$0.0000 + 0.0000i$
b_0	$1.0 + 0.0i$	$2.3667 + 1.0000i$	$0.1509 + 0.0283i$	$3.0667 + 1.4000i$
c_0	$2.2 + 0.1i$	$2.2000 + 0.1000i$	$2.2000 + 0.1000i$	$2.2000 + 0.1000i$
a_1	$0.5 + 0.3i$	$0.8833 + 1.2100i$	$0.0670 + 0.0594i$	$1.1133 + 1.6200i$
b_1	$0.4 - 0.7i$	$0.7833 + 0.2100i$	$-0.0330 - 0.9406i$	$1.0133 + 0.6200i$
a_2	$0.3 - 0.3i$	$1.0100 - 0.4100i$	$0.0538 - 0.0368i$	$1.3400 - 0.5000i$
b_2	$0.4 + 0.5i$	$0.2867 - 0.3933i$	$0.7213 + 0.8176i$	$0.1853 - 0.8099i$
a_3	$0.2 - 0.7i$	$0.1000 - 0.5000i$	$0.2828 - 1.2069i$	$-0.1793 - 0.8517i$
b_3	$-0.5 + 0.3i$	$0.3353 + 0.5412i$	$-0.5828 + 0.8069i$	$0.6146 + 0.8929i$
a_4	$0.6 + 0.3i$	$-0.5533 - 0.0067i$	$1.0450 + 0.4610i$	$-0.8726 + 0.3616i$
b_4	$-0.1 + 0.5i$	$-0.2000 + 0.7000i$	$0.1793 + 0.8517i$	$-0.2828 + 1.2069i$
a_5	$-0.6 + 0.3i$	$-0.6000 + 0.3000i$	$-0.7966 - 0.5586i$	$-0.7966 - 0.5586i$
b_5	$0.7 + 0.3i$	$0.8941 - 0.3235i$	$-0.8966 - 1.6586i$	$-1.8260 - 1.4763i$
a_6	$0.2 + 0.0i$	$0.4733 + 0.2000i$	$0.0302 + 0.0057i$	$0.6133 + 0.2800i$
a_7	$-0.3 - 0.5i$	$-0.3000 - 0.5000i$	$-0.3000 - 0.5000i$	$-0.3000 - 0.5000i$
a_8	$-0.1 - 1.1i$	$-1.0294 - 0.9176i$	$1.3000 + 0.0000i$	$1.4941 - 0.6235i$
a_9	$-0.9 - 0.1i$	$-0.9000 - 0.1000i$	$-0.9000 - 0.1000i$	$-0.9000 - 0.1000i$
b_9	$0.6 + 0.5i$	$0.6000 + 0.5000i$	$0.6000 + 0.5000i$	$0.6000 + 0.5000i$

4 Show Completeness

We have shown how to find all permutation cognates. It is much harder to show that no other type of cognate exists. To attack this problem, we solve a special type of precision-point path synthesis problem. For four-bars, one could settle the question by sampling ten general points from the coupler curve of a general four-bar, solving a path synthesis problem for nine of these points, and checking which of these solutions also interpolates the tenth point. This would give the original linkage and all its cognates. For four-bars, this is feasible, but for a six-bar, this would require solving a path synthesis problem having 15 precision points which is beyond current computational capability.

Fortunately, by taking advantage of focal information, we can bring the six-bar problems within range. We can compute the singular foci and use their signature to derive symbolic expressions for them. As one may see in Table 2, these focal equations are much simpler than the coupler curve equation. So instead of all general points, it is easier to solve a path synthesis problem whose precision points are the singular foci and a sufficient number of additional general points. As an example, consider specifying singular foci F_1, F_2, F_3 for the four-bar. Then, Table 2 tells us that $a_0 = F_1$, $b_0 = F_2$, and

$$F_1 a_2 + (F_2 - F_1) b_2 = F_3 a_2$$

These three conditions and their conjugate counterparts ($\bar{a}_0 = \bar{F}_1$, etc.) are six independent linear conditions. Consequently, the determination of all four-bar path cognates can be accomplished by adding just three more general precision points and then checking the solutions against a fourth one. This is much simpler than solving a nine-point problem.

For six-bars, we proceed similarly. The first step is to check how many independent conditions are imposed by specifying the singular foci. Let x be the set of link parameters, $x = (a_0, b_0, \ldots)$, and suppose that $S(x)$ is map that gives the singular foci. Choose a general (i.e., random) set of parameters x^*. Then, all cognates to x^* must satisfy $S(x) - S(x^*) = 0$. Let $JS(x^*)$ be the Jacobian matrix of S evaluated at x^*. By Ref. [20], assigning the singular foci imposes rank $JS(x^*)$ conditions on the link parameters. Accordingly, we only need to specify $k = 15 - \text{rank}\, JS(x^*)$ additional precision points to obtain an exactly constrained path synthesis problem. The k points are randomly sampled from the original coupler curve to ensure genericity. The second column in Table 5 lists k, the remaining degrees-of-freedom, for the four-bar and six-bar linkages.

When forming the path synthesis problems, for the four-bars and six-bars, we may write the j^{th} entry of $S(x)$ form $S_j(x) = p_j(x)/q_j(x)$. Clearing the denominator yields a polynomial of the form $p_j(x) - S_j(x^*) \cdot q_j(x) = 0$ for each singular focus.

Methods in numerical algebraic geometry [12,14] can be used to both sample random points from the coupler curve and solve the resulting path synthesis problem for four-bar and six-bar linkages. In particular, our experiments utilized regeneration [23,24] to solve the path synthesis problems with the resulting finite number of nondegenerate linkages summarized in Table 5.

Due to degrees-of-freedom counting, each nondegenerate linkage is a cognate of the original linkage if its coupler curve also passes through one additional randomly selected point on the coupler curve. If this additional check results in a unique cognate linkage, then the completeness test verifies that there is indeed a unique cognate per valid assignment of singular foci. This was indeed the case for the four-bar (confirming Roberts's result [1]) and the Stephenson-3 (confirming Roth's result [7]). The same was true for the Watt-1B, Stephenson-1, Stephenson-2A, and Stephenson-2B six-bar linkages which proves that Dijksman's corresponding list of cognates is complete.

For the Watt-1A, Sec. 3.7 states that there is only the trivial assignment of the singular foci and there is a two-dimensional family of cognates. One natural way to parameterize this two-dimensional family is by the ground pivot a_0 which, in isotropic coordinates, corresponds with the two variables $(a_0, \bar{a}_0)$. Hence, one first fixes this ground pivot and then applies the completeness test to verify that there indeed is a unique cognate proving that Dijksman's corresponding list of cognates is complete. We note that this computation first required the filtering of degenerate components before checking at an additional random point on the coupler curve.

Table 5 Number of points on the coupler curve (k), which is the degrees-of-freedom after specifying the singular foci, and number of nondegenerate solutions of the k-point problem after specifying the singular foci

Mechanism	k points	# solutions
4-Bar	3	4
Watt-1A	5	958
Watt-1B	2	34
Stephenson-1	2	32
Stephenson-2A	5	3344
Stephenson-2B	5	3472
Stephenson-3	5	3430

5 Conclusion

Permutation cognates are those that arise by permuting link rotation angles. Dijksman conjectured that all planar cognates are permutation cognates and compiled a list of them for all six-bar planar mechanisms. He did not show how to make sure the list is exhaustive or how to generalize his approach to higher-order linkages. We have shown that analyzing the vanishing rotations corresponding to the singular foci of a mechanism type produces a short list of permutations that are compatible with preserving these focal signatures. This reproduces the result known for four-bars and also reproduces Dijksman's list for six-bars, confirming that he found all permutation cognates. Testing an eight-bar example, our method reveals that just one nontrivial permutation preserves the focal signatures, and indeed, it yields a path cognate. For a ten-bar example, our method reveals that three independent transpositions of rotations preserve the focal signatures, but the further step of deriving cognates using these transpositions shows that one of them is inconsistent. Thus, this linkage type is shown to have exactly four permutation cognates (counting the original linkage).

Since its ground link is fixed, an n-bar linkage has $(n-1)!$ possible ways to permute its rotations. Restricting one's search to just permutation cognates, our method provides an extreme reduction in the number of permutations to check compared to a naive approach of checking all possible permutations. For the eight-bar we studied, the reduction is from $7! = 5040$ to just one transposition. For the ten-bar, it reduces the cases from $9! = 362{,}880$ to just three transpositions.

For six-bars, we were able to check Dijksman's Conjecture by computing all cognates that match a given assignment of singular foci by adding to the focal conditions a minimally sufficient number of precision points sampled generically from the coupler curve and solving the resulting path synthesis problem. Without the focal conditions, one would be faced with a 15-point path synthesis problem, which is currently impossible to solve completely. With the focal conditions, one needs to add only two or five precision points (depending on the linkage type). These smaller problems are feasible, and we find in every case that only permutation cognates result. This confirms Dijkman's Conjecture for general six-bars, confirming that the list of permutation cognates is in fact the complete list of all possible path cognates.

While our methodology has proven effective for finding all permutation cognates for higher-order linkages, we are presently not able to solve the path synthesis problems that would confirm Dijksman's Conjecture for eight-bars or beyond due to computational limitations.

Acknowledgment

SNS and JDH were partially supported by NSF CCF-181274. SNS was also supported by the Schmitt Leadership Fellowship in Science and Engineering.

Conflict of Interest

There are no conflicts of interest.

References

[1] Roberts, S., 1875, "On Three-Bar Motion in Plane Space," Proc. Lond. Math. Soc., **7**(1), pp. 14–23.
[2] Dijksman, E., 1976, *Motion Geometry of Mechanisms*, Cambridge University Press Archive, Cambridge.
[3] Dijksman, E., 1971, "Six-Bar Cognates of Watt's Form," J. Eng. Ind., **93**(1), pp. 183–190.
[4] Dijksman, E., 1971, "Six-Bar Cognates of a Stephenson Mechanism," J. Mech., **6**(1), pp. 31–57.
[5] Nolle, H., 1974, "Linkage Coupler Curve Synthesis: A Historical Review- II. Developments After 1875," Mech. Mach. Theory, **9**(3–4), pp. 325–349.
[6] Nolle, H., 1974, "Linkage Coupler Curve Synthesis: A Historical Review-I. Developments Up to 1875," Mech. Mach. Theory, **9**(2), pp. 147–168.
[7] Roth, B., 1965, "On the Multiple Generation of Coupler Curves," Trans. ASME, Ser. B J. Eng. Ind., **87**(2), pp. 177–183.
[8] Sherman, S. N., Hauenstein, J. D., and Wampler, C. W., 2020, "Curve Cognate Constructions Made Easy," Proceedings of the ASME 2020 International Design Engineering Technical Conferences and Computers and Information in Engineering Conference, Virtual, Online.
[9] Sherman, S. N., Hauenstein, J. D., and Wampler, C. W., 2021, "A General Method for Constructing Planar Cognate Mechanisms," ASME J. Mech. Rob., **13**(3), p. 031107.
[10] Wampler, C. W., 2004, "Singular Foci of Planar Linkages," Mech. Mach. Theory, **39**(11), pp. 1123–1138.
[11] Wampler, C. W., 2004, "The Geometry of Singular Foci of Planar Linkages," Mech. Mach. Theory, **39**(11), pp. 1139–1153.
[12] Sommese, A. J., and Wampler, C. W., 2005, *The Numerical Solution of Systems of Polynomials Arising in Engineering and Science*, World Scientific, Singapore.
[13] Bates, D. J., Hauenstein, J. D., Sommese, A. J., and Wampler, C. W., 2006, "Bertini: Software for Numerical Algebraic Geometry," bertini.nd.edu
[14] Bates, D. J., Hauenstein, J. D., Sommese, A. J., and Wampler, C. W., 2013, *Numerically Solving Polynomial Systems with Bertini*, Vol. 25, Society for Industrial and Applied Mathematics (SIAM), Philadelphia, PA.
[15] Wampler, C. W., Morgan, A., and Sommese, A. J., 1992, "Complete Solution of the Nine-Point Path Synthesis Problem for Four-Bar Linkages," ASME J. Mech. Des., **114**(1), pp. 153–159.
[16] Morgan, A. P., and Wampler, C. W., 1989, "Solving a Planar Four-bar Design Problem Using Continuation," Proceedings of the ASME 1989 Design Technical Conferences, Montreal, Quebec, Canada, pp. 409–416.
[17] Coolidge, J., 1959, *A Treatise on Algebraic Plane Curves*, Dover, New York.
[18] Bottema, O., and Roth, B., 1990, *Theoretical Kinematics*, Dover, New York.
[19] Wampler, C., 2001, "Solving the Kinematics of Planar Mechanisms by Dixon Determinant and a Complex-Plane Formulation," ASME J. Mech. Des., **123**(3), pp. 382–387.
[20] Hauenstein, J. D., and Sommese, A. J., 2010, "Witness Sets of Projections," Appl. Math. Comput., **217**(7), pp. 3349–3354.
[21] Bates, D. J., Hauenstein, J. D., McCoy, T. M., Peterson, C., and Sommese, A. J., 2013, "Recovering Exact Results From Inexact Numerical Data in Algebraic Geometry," Exp. Math., **22**(1), pp. 38–50.
[22] Choe, J., Li, D., Soh, G., and McCarthy, J. M., 2009, "Synthesis of a 10-bar Driver for Planar Scale Change Linkages," 2009 ASME/IFToMM International Conference on Reconfigurable Mechanisms and Robots, London, UK, pp. 142–147.
[23] Hauenstein, J. D., Sommese, A. J., and Wampler, C. W., 2011, "Regeneration Homotopies for Solving Systems of Polynomials," Math. Comp., **80**(273), pp. 345–377.
[24] Hauenstein, J. D., and Wampler, C. W., 2017, "Unification and Extension of Intersection Algorithms in Numerical Algebraic Geometry," Appl. Math. Comput., **293**(1), pp. 226–243.